

## Aperiodicity in Bowed-String Motion

by M. E. McIntyre

Department of Applied Mathematics and Theoretical Physics, Silver Street,  
Cambridge, CB3 9EW

R. T. Schumacher

Department of Physics, Carnegie-Mellon University, Pittsburgh, Pa. 15213

and J. Woodhouse

Topexpress Ltd., 1 Portugal Place, Cambridge, CB5 8AF

### Summary

An investigation of the causes of aperiodicity in bowed-string oscillations is made using simple experiments, theoretical arguments and computer simulations, and the status of theoretical models which idealise the behaviour as exactly periodic is thus assessed. Three distinct sources of departures from a strictly periodic Helmholtz-like motion are studied.

First, careful measurements of "flyback jitter" in the bridge-force waveform, reflecting variation in the timing of the round trip of the Helmholtz corner, are made. They reveal that when extraneous effects are minimised this type of jitter is apparently too small to be audible, contrary to earlier observations. Such variation as is observed appears to arise from externally-imposed irregularities, for example in the distribution of rosin on the bow-hair.

The second source of departures from Helmholtz periodicity is the excitation of sub-harmonic perturbations, whose existence and behaviour can best be appreciated from the characteristic space-time diagram for a string carrying a Helmholtz motion. If losses are sufficiently small and reflection from the bow during sticking sufficiently strong, negative resistance at the bow during slipping causes such sub-harmonic perturbations to become self-excited; this is shown to be the physical mechanism underlying an instability discovered mathematically by Friedlander. The sub-harmonic mechanism appears to be more important for understanding the behaviour of idealised models than for understanding that of real strings under normal playing conditions.

The third source of aperiodicity, which appears to be musically the most important since it gives rise to clearly audible noise under some conditions encountered in normal violin playing, is shown to be associated with differential slipping of the bow hairs during the normal sticking phase of the Helmholtz cycle. A characteristic signature of this noisy regime is the appearance of sharp "spikes" in the bridge-force waveform. The average timing and amplitude of the spikes are sensitive to bow force and friction characteristics, and the results suggest ways of measuring friction characteristics under the conditions of actual playing.

### *Aperiodizität in der Bewegung der gestrichenen Saite*

### Zusammenfassung

Eine Untersuchung der Ursachen von Aperiodizitäten in Schwingungen gestrichener Saiten wurde anhand einfacher Experimente, theoretischer Überlegungen und Computersimulationen durchgeführt. Auf diese Weise wurde die Qualität der theoretischen Modelle, welche das Verhalten der Saite als exakt periodisch annehmen, abgeschätzt. Drei unterschiedliche Ursachen für die Abweichungen von einer streng periodischen Helmholtzschwingung wurden untersucht.

Zunächst wurden sorgfältige Messungen des „flyback jitter“ in der Schwingung der Stegkraft durchgeführt, welcher die Variationen in der Zeitabfolge von Umläufen der Helmholtzstelle widerspiegelt. Sie offenbaren, daß im Falle minimalisierter Nebeneffekte diese Art von „jitter“ anscheinend zu klein ist, um hörbar zu sein, was im Gegensatz zu früheren Beobachtungen steht. Variationen, wie die beobachteten, scheinen durch von außen eingebrachte Unregelmäßigkeiten zu entstehen, wie z.B. die Verteilung des Kolophoniums auf den Bogenhaaren.

Die zweite Ursache für Abweichungen von der periodischen Helmholtzschwingung ist die Anregung von subharmonischen Störungen, deren Existenz und Verhalten am besten anhand des charakteristischen Raum-Zeit-Diagramms der Helmholtzschwingung einer Saite abgeschätzt werden kann. Ist der Verlust genügend klein und die Reflexion am Bogen während der Haftung genügend groß, bewirkt der negative Widerstand des Bogens während des Gleitens die Selbsterregung solcher subharmonischen Störungen. Es wird gezeigt, daß diese Wirkung der von Friedlander mathematisch entdeckten Instabilität zugrundeliegt. Der subharmonische Mechanismus scheint bedeutender für das Verständnis des Verhaltens idealisierter Modelle zu sein als für das Verständnis des Verhaltens realer Saiten bei normalen Spielbedingungen.

Die dritte Ursache für Aperiodizitäten scheint musikalisch die bedeutendste zu sein, da sie zu deutlich hörbarem Geräusch führt, welches manchmal beim normalen Violinspiel auftritt. Es hat sich gezeigt, daß sie in Zusammenhang mit teilweisem Schlupf der Bogenhaare während der Haftphase des Helmholtzzyklus steht. Eine charakteristische Eigenart dieser geräuschvollen Form ist das Erscheinen von schmalen Nadeln in der Schwingung der Stegkraft. Die durchschnittliche Zeitabfolge und Amplitude der Nadeln ist abhängig von der Bogenkraft und der Reibungskennlinie. Die Ergebnisse zeigen Möglichkeiten auf, die Reibungskennlinie während des normalen Spiels zu messen.

*L'apériodicité du mouvement de la corde frottée*

Sommaire

On a recherché les causes qui rendent apériodiques les oscillations d'une corde frottée, en s'appuyant soit sur des expériences simples, soit sur des arguments théoriques, soit encore sur des simulations numériques. On remet ainsi en cause les modèles théoriques qui supposent un comportement strictement périodique de la corde. Trois raisons distinctes ont été identifiées et étudiées comme susceptibles d'entraîner des écarts à un mouvement strictement périodique à la Helmholtz.

Tout d'abord on a effectué des mesures soignées du «flyback jitter» (saccade de retour rapide) au niveau de la force exercée sur le chevalet, où l'on a observé des variations dans le temps de retour du sommet anguleux du profil ondulatoire à la Helmholtz. Ces mesures ont révélé que, contrairement à des observations antérieures, cet effet de jitter est trop faible pour être audible, pourvu qu'on arrive à éliminer, ou du moins à minimiser, certaines causes étrangères, comme celles qui peuvent provenir d'une distribution irrégulière de la colophane sur la mèche de l'archet.

La seconde origine possible d'un écart à la périodicité d'un mouvement à la Helmholtz est l'excitation de perturbations sous-harmoniques. Le meilleur moyen de vérifier leur existence et apprécier leur comportement est l'étude du diagramme caractéristique en espace-temps pour une corde supportant un mouvement à la Helmholtz. Si l'on suppose assez faible la dissipation et assez forte la réflexion par l'archet durant la phase d'adhérence, on trouve que la résistance négative de l'archet pendant la phase de glissement sera effectivement la cause d'une auto-excitation de telles perturbations sous-harmoniques. Ceci peut être considéré comme le mécanisme physique d'une instabilité découverte mathématiquement par Friedlander. Cependant ce mécanisme de sous-harmonicité paraît plus important pour la compréhension du comportement des modèles idéalisés que pour saisir celui d'une corde réelle dans les conditions instrumentales normales.

La troisième cause d'apériodicité, du point de vue musical sans doute la plus importante, puisqu'elle occasionne un bruit nettement audible dans certaines conditions d'un jeu normal du violon, est associée, comme on le montre ici, à un glissement différentiel des crins de l'archet durant la phase nominale d'adhérence dans le cycle de Helmholtz. Une signature caractéristique de ce régime est l'apparition de pointes aiguës dans le diagramme ondulatoire de la force sur le chevalet. L'amplitude et la cadence moyennes d'apparition de ces pointes dépendent de la force d'application de l'archet et des caractéristiques du frottement de l'archet sur la corde, résultat qui suggère des voies nouvelles pour mesurer ces caractéristiques dans les conditions d'un jeu normal.

1. Introduction

Oscillations maintained by the action of non-linearity of some kind are common, and have been widely studied. However, whereas the usual concern of the engineer investigating squeaking brakes or fan flutter in turbines is simply how to control or prevent such oscillations, the musical acoustician has a harder problem. To investigate vibrations in a wind instrument or a bowed-string instrument in a way which has relevance to the musician necessitates studying details, sometimes very fine details, of the behaviour of the system in question [1].

Our concern here is with the bowed string. In two recent articles [2], [3] we have established a very general framework for studying this problem, which incorporates and extends previous work on the subject, especially the fundamental work of refs.

[4], [5], [6]; and we have examined some questions of direct musical interest not previously investigated. Much of the work cited concentrates on periodic motion of the string, and especially on variation of the waveform and frequency of the basic "Helmholtz" motion as one moves around in the appropriate part of bowing parameter space.

In further pursuit of those musically all-important details, we now ask whether all (or indeed any) regimes of musical interest can in fact be described to sufficient accuracy as periodic motions. There are three lines of evidence suggesting that this might not be so: one experimental, one arising from early work on mathematical modelling and a third readily apparent to the ear. We discuss all three in this paper, with the intention of giving a connected account of what kinds of cycle-by-cycle variation are possible during "steady" playing.

The first line of evidence on aperiodicity comes from measurements of the variations in period lengths of successive cycles of bowed-string waveforms [6], [7]. These measurements have been reported as showing a distribution with a standard deviation of some 7 cents (a cent is a hundredth of an equal-tempered semitone, in other words a frequency ratio of  $1200/\sqrt{2} \cong 1.0006$ ); we should note in this connection that psychoacoustical measurements [8] suggests a threshold for perception of jitter (in headphones) of about 5 cents' standard deviation for normally-distributed period lengths. It has furthermore been suggested [6] that the observed "jitter" may in some way be intrinsic to bowed string dynamics. The latter idea challenges the theoretical validity of idealising bowed-string motion as periodic, and merits investigation.

The second line of evidence comes from the mathematical work of Friedlander [9], who studied what is perhaps the simplest model of the bowed string, namely an ideal, nondissipative "textbook" string with rigid terminations, bowed at a single point dividing the string in a rational ratio. He found, among other interesting things, that for this model all periodic motions are unstable. This discovery again merits further investigation, since it too could be indicative of an intrinsic tendency toward aperiodicity in bowed-string motion.

The third line of evidence is the marked build-up of audible noise accompanying the musical note when trying to play more and more loudly near the bridge. Indeed one of the ways in which limits on usable bowing parameters are determined in practice is by this noise becoming unacceptably great for the musical context. It is natural to ask whether the aperiodicity associated with this noise has any connection with the jitter already reported or with Friedlander's instability. In that case the jitter or instability would have to depend strongly on one's position in bowing parameter space, as does the audible noise. Alternatively, the audible noise might have some entirely different source. In any case this question, too, deserves closer investigation.

Concerning the first line of evidence (jitter measurements), previous reports did not contain much information about the detailed circumstances under which the measurements were made, in particular about what type of playing was employed and thus to what part of bowing parameter space they were supposed to apply. We therefore start this investigation (section 2) by very carefully repeating those measurements to see whether there are any regions of parameter space within the tolerance limits of normal playing where it seems reasonable to idealise the motion as periodic. We find that the

jitter is smaller, usually much smaller, than previously reported. From these results together with simple theoretical considerations (which seem to account rather well for the observed behaviour) we conclude that jitter is not, in fact, intrinsic to bowed-string dynamics.

We then examine in detail, both experimentally and theoretically, the implications of the second and third lines of evidence and the extent of their connection with the first. The second line of evidence, Friedlander's instability, is discussed in section 3. We show by a simple graphical construction that the instability in the ideal-string model takes the form of sub-harmonics of the note being played, which grow exponentially in time. It turns out that real, in practice strings do not suffer from the instability as such, for reasons to be explained. Nevertheless sub-harmonic behaviour, albeit not self-excited, can be observed under certain transient conditions in real strings. The sub-harmonic mechanism cannot by itself account for the observed jitter, but it probably affects the statistical properties of the jitter to some degree.

The third line of evidence, the noise accompanying loud notes played near the bridge, is found to be connected neither with jitter (as measured here) nor with the sub-harmonic mechanism. Rather, the aperiodicity causing the noise turns out to be an entirely separate phenomenon in which an essential role is played by the finite width of bow-hair in contact with the string. A combination of experiment, theory and computer simulation not only yields a convincing explanation of this noise and its parameter dependence (section 4), but suggests methods of measuring frictional characteristics under dynamical conditions close to those of normal playing (section 5). Such measurements have apparently not been made; the only measurements of rosin friction of which we are aware were for constant relative velocity only [10], and it is not known how well those results apply to actual playing conditions.

When we come to check our ideas by computer simulations of string motion, we have two basic models to draw on. One is the Raman model, which is the generalisation of the model used by Friedlander in which the string, still ideally flexible, has pure-resistive terminations to provide some dissipation. The second is the rounded-corner model which we have described previously [2], a development of the work of Cremer and Lazarus [6]. It combines excellent computational efficiency with allowance for very realistic behaviour of the string and its terminations, including the rounding of the Helmholtz corner or velocity jump. Such realistic be-

haviour is not allowed for in the Raman model. The rounded-corner model assumes only that the string and terminations behave linearly, so that bow-friction is the only nonlinearity. We have implemented both models on a minicomputer to perform fully transient simulations which can be "played": that is to say bowing parameters can be varied from the computer keyboard during the run, enabling transient behaviour, stability etc. to be investigated, as well as stable periodic motion. These programs give a very versatile means of studying the models, especially since some vibration regimes are accessible, as in real violin playing, only from a starting transient during which bowing parameters are varied in a particular way.

For some of our experimental observations we used strings mounted on a violin of no particular pedigree (albeit with some high-class concert experience). The remaining experiments used a monochord based on an optical bench.

## 2. Measurements of flyback jitter

We first discuss our attempt to repeat as accurately as possible the previous measurements of period lengths of successive cycles of a bowed string waveform. To do this we took advantage (as did Cremer [6]) of the very steep slope generated in the waveform of transverse force at the bridge when the Helmholtz corner reflects there. For an ideal string the force waveform is a sawtooth with a vertical "flyback", and on real strings it is more or less close to this. An example is given in Fig. 1, from a thin metal string on a monochord; the marked portion occupies some 2% of the total-period length in this case. Again as in ref. [6], we observe force at the bridge by means of a piezoelectric transducer previously described by Reinicke [11], and kindly supplied by him.

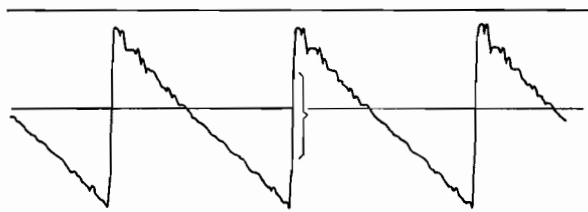


Fig. 1. Typical bridge-force waveform of a thin metal string on a monochord, bowed by hand with a normal bow. In the jitter-measurement program, the position of each zero-crossing is determined from a suitable (sufficiently straight) portion of the flyback, such as that marked in the figure, chosen before each run by inspection of one cycle of the waveform.

In the jitter experiments, strings mounted on both a monochord and a violin were bowed by hand, mezzo-forte, using an ordinary bow. The bridge-force signal was digitised, and for each "take", 23000 values were read into the memory of the minicomputer (an Alpha LSI-2) at a sampling rate of up to 160 kHz. Then the positions of the steep zero-crossings in this stored signal were computed by fitting a least-squares straight line to the measured points in the centre of the flyback-portion (as indicated in Fig. 1) to minimise sampling in-

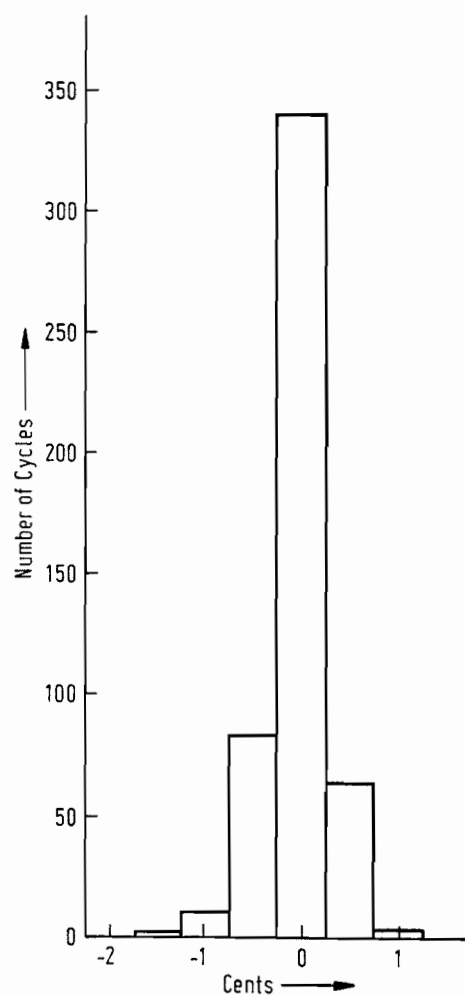


Fig. 2. Jitter histogram for the thin metal string on the monochord, bowed by hand with a normal bow. The string was 0.007 inch diameter "rocket wire" (high-tensile steel), with length 450 mm, tuned to 652 Hz. The fractional distance  $\beta$  of the bow from the bridge was about 0.1 and the bow speed was approximately 0.4 m/s. Occurrences of a given deviation from nominal pitch are collected in 1/2-cent bins. Positive deviation corresponds to higher pitch, or shorter period. The standard deviation of the distribution is 0.4 cent.

accuracies, enabling frequencies to be calculated to an accuracy of better than 1/2 cent for low-register violin notes. The instantaneous frequencies (inverse periods) were displayed cycle by cycle, and the number of occurrences of a given deviation from nominal frequency collected in histograms with a resolution of 1/2 cent. The spread of periods measured in this way we call "flyback jitter", to distinguish it from other sources of aperiodicity which might contribute to the spread of period lengths if a different measurement technique were used (for example using zero-crossings in a microphone signal of radiated sound, rather than bridge-force).

Our results are at variance with those previously reported. To take the most extreme example first, the thin, very flexible metal string mounted on a monochord (waveform typified by Fig. 1) produced the histogram shown in Fig. 2 when bowed lightly, not far above minimum bow-force [5] (see caption for further details). It is plain that the total spread of frequencies is not much above 1 cent, so small that it can reasonably be attributed to measurement errors, in conjunction with the irregularities inevitable with hand bowing. The standard deviation in Fig. 2 is 0.4 cent, or about 0.0002 of a period. On occasion we have managed to produce as many as 36 consecutive cycles equal in frequency to within 1/2 cent, with this string. It seems plausible that this string at least would be capable of precisely periodic motion if exactly steady bowing conditions prevailed.

It should be emphasised that great care is needed to avoid spurious results when measuring periods to this accuracy, as there are many sources of additional spread in the histogram which must be minimised. With a metal string, the slightest fluctuations in bow-force or vibration amplitude can produce pitch changes of more than a cent, owing to changes of tension in the string. Also, if stopped notes on an instrument are being measured, the warmth of the player's finger will induce a downward drift of several cents over a few seconds as the measurement proceeds. Other sources of irregularity or systematic drift of frequency stem from the inevitable slight variations in bowing parameters: they include the pitch-flattening effect discussed elsewhere [2], [3] (which is sensitive to bow force since it arises from hysteresis in the capture-release process at the bow-string contact), and the transient excitation of sub-harmonics, to be discussed in the next section. It should be emphasised that in normal playing these effects may all be present to some degree, and the actual spread of periods under such circumstances may sometimes be as high as the previous measurements suggest. At present we are

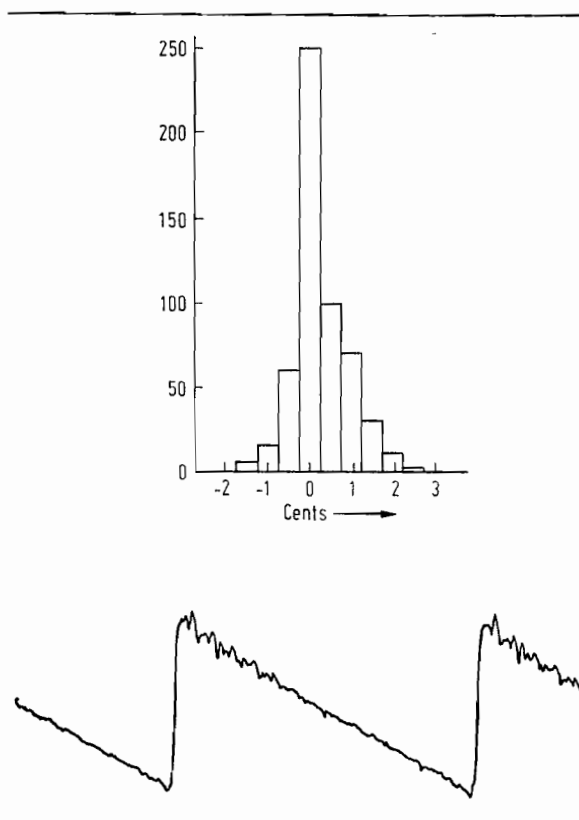


Fig. 3. Jitter histogram and sample of bridge-force waveform for a violin open (i.e. unstopped) steel *E* string (660 Hz), bowed by hand with a normal bow. The bowing point  $\beta$  is about 1/15, and the bow speed about 0.4 m/s. The standard deviation of the distribution is 0.7 cent.

concerned to know to what extent periodic motion is possible when these additional effects are minimised.

Some of these additional effects would appear at first sight to produce not true cycle-by-cycle jitter (which we do indeed observe) but only changes on longer time-scales. However it should be remembered that although the longer-time-scale changes are certainly present, any change also evokes a small amount of transient response in the string, so that some cycle-by-cycle variation also arises.

Flyback-jitter histograms for other strings, now mounted on the violin, are shown in Figs. 3 to 6. In each case, a sample of the bridge-force waveform is also shown. In all cases, bow-force was just above minimum and bow speed much the same as before. Standard deviations are given in the captions. Thicker strings are seen to be more prone to jitter than thinner ones, but even for high stopped notes on a violin *G* string (stopped with a rubber "artificial finger"), flyback jitter is at least a factor

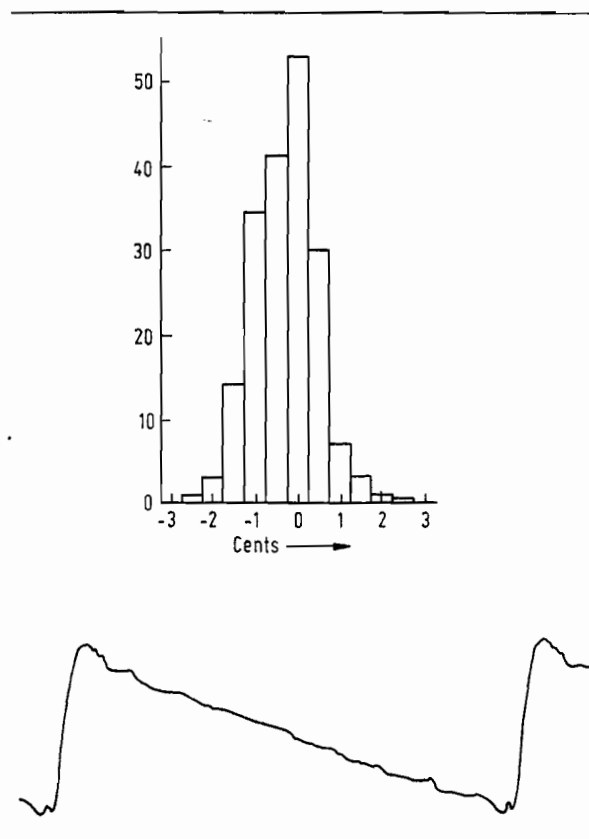


Fig. 4. Jitter histogram and sample of bridge-force waveform for a violin open *G* string (196 Hz), bowed by hand with a normal bow. The *G* strings used in all our experiments with the violin were ordinary, silver-wound gut strings. Bowing parameters were similar to those of Fig. 3. The standard deviation of the distribution is 0.8 cents.

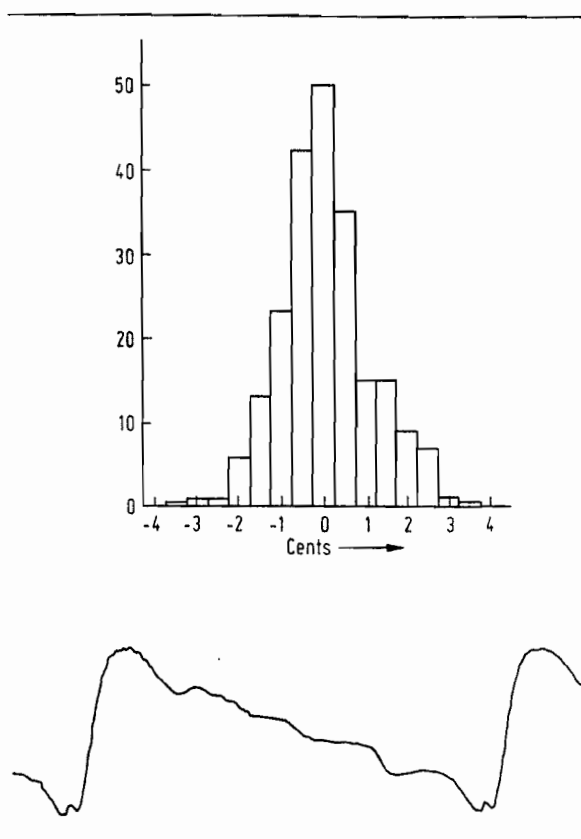


Fig. 5. Jitter histogram and sample of bridge-force waveform for a violin *G* string stopped (with a soft rubber eraser) at 305 Hz and bowed by hand with a normal bow. Bow speed was still about 0.4 m/s, and  $\beta \cong 0.19$ . The standard deviation of the distribution is 1.1 cent.

2 below the nominal audibility threshold of a standard deviation of some 5 cents [8].

These observations seem to be consistent with a very simple explanation of flyback jitter. The rosin on the bow-hair will inevitably not be quite uniformly distributed, and bow-hairs themselves are far from homogeneous along their lengths, as is shown by scanning electron micrographs [12] (although bow-hairs do not possess the barbed structure popularly supposed). Thus the friction characteristics, and in particular the effective value of the coefficient of sticking friction, will vary from point to point of the hair. The extent of this variation has not to our knowledge ever been measured, but it is clear that flyback jitter will result, bearing in mind the discussion of refs. [6], [5] and [2] relating to the interaction of a rounded Helmholtz corner on the string with friction at the bow. The precise moment at which the string is captured or released by the bow when a rounded Helmholtz corner arrives depends critically on the details of the friction characteristic for velocities close to sticking.

Jitter arising from this mechanism will clearly be more or less proportional to the roundedness of the Helmholtz corner, given by the time occupied by the flyback in the bridge-force waveform as a fraction of the total period length. (In addition we should note that the resolution of the measurement technique increases as the steepness of the flyback.) Thus measured flyback jitter should indeed increase in going from thinner to thicker strings, since the corner becomes more rounded and hence the flyback less steep. Possible reasons for the change in roundedness include increased dispersive effects arising from larger diameters, stronger coupling of lower strings of an instrument to the body, and an increase in high frequency damping arising from the internal structure of wound strings; see ref. [2] for further discussion and references. Flyback jitter expressed in fractions of a period should also increase upon moving to higher positions on a given string, since the flyback time will remain roughly constant while the period decreases. Both of these effects are clearly visible in the waveform pictures

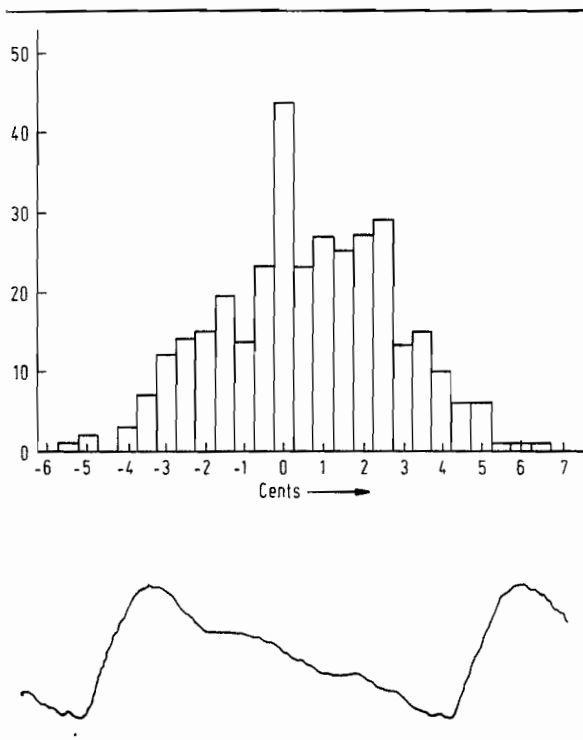


Fig. 6. Jitter histogram and sample of bridge-force waveform for a violin *G* string stopped at 715 Hz (near the end of the fingerboard) and bowed by hand with a normal bow. Bow speed was still about 0.4 m/s, and  $\beta \approx 0.3$ . The standard deviation of the distribution is 2.3 cent.

accompanying the jitter histograms. In particular, Fig. 2 (showing jitter on the limit of the resolution of the measurement technique) was obtained using a string whose flyback in the bridge-force waveform (illustrated in Fig. 1) occupied only about 0.05 ms, about 3% of the total period length. The opposite extreme comes in Fig. 6, where high on the *G* string, the flyback takes about 0.3 ms and occupies about 20% of the period length. The corresponding amounts of jitter are indeed roughly in proportion.

Our proposed mechanism for flyback jitter is further supported by experimental evidence (omitted here for brevity) that there is little variation of jitter within the normal tolerance range in bowing parameter space. It is known from previous investigations [6], [2], [3] that corner-rounding decreases as bow force is increased, so that we would perhaps expect a slight decrease in jitter as force is increased. However, the other factors causing a spread of periods tend to increase as force is increased so that experimental uncertainties increase, and the net effect on the observed spread is in fact very slightly upward. Computer simulations using the rounded-corner model of ref. [2] have also been made, in which normal bow-force was randomly varied from time step to time step to imitate a fluctuating

friction characteristic. The jitter arising in the simulations behaved quite similarly to that in the measurements.

One noteworthy outcome of the measurements was that even during the audibly noisy loud playing of a musical note with the bow near the bridge, flyback jitter was never much greater than shown in Figs. 2 to 6, well below the nominal threshold for direct audibility. Thus flyback jitter cannot account for the marked build-up of audible noise as bow-force is increased and distance to the bridge reduced. We identify the cause of that noise in section 4 after we have dealt, in the next section, with another interesting phenomenon, which shows up in some of the cycle-by-cycle jitter observations (although it was first detected by ear) and which turns out to be intimately connected with the mechanism of Friedlander's instability.

To summarise so far it seems reasonable to conclude, subject to experimental verification that bow and rosin non-uniformities are in fact of the right order, that the observed flyback jitter is due entirely to such non-uniformities and is not inherent in the basic bowed string mechanism. The jitter observations do not invalidate the traditional assumption that we can learn a substantial amount about the bowed string through theories assuming periodic motion.

### 3. "Ghostly sub-harmonics" and Friedlander's instability

In the course of careful listening to certain of the more extreme regimes of bowed-string vibration, it was noticed that a faint sub-harmonic of the note being played could sometimes be heard as well as the note itself. The order of this sub-harmonic depended on the position  $\beta$  of the bow as a fraction of string length. We are not here talking about the variety of raucous, sub-fundamental frequencies produced when bow-force exceeds Schelleng's maximum [5], but a very faint sub-octave, twelfth, etc. heard while playing an ostensibly normal Helmholtz motion at the natural pitch of the string, and sometimes apparent to the ear only after listening for a minute or so. The audible impression made by these sounds is not of a clear, steady note; rather, they have an irregular, indefinite character somewhat like the response of a cavity to random-noise excitation. Hence we christened the sounds "ghostly sub-harmonics". The effect is best demonstrated by stopping a violin *E* string (with the finger, in the usual way) high up and playing with rather large bow-force and slow bow speed. Care should be taken that the sub-harmonic listened to does not

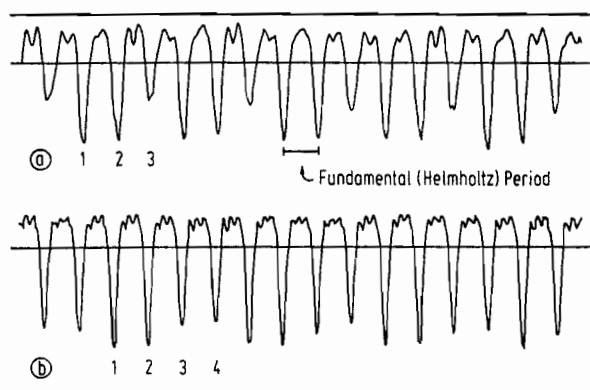


Fig. 7. String velocity observed near the bowing point showing the presence of sub-harmonics, obtained by bowing with an ordinary bow a violin *E* string stopped at 1730 Hz (around top A). The magnet method of [5] was used to observe string velocity, and bow-force was near maximum. Case (a), with  $\beta \cong 1/3$ , shows a prominent third subharmonic, in which the pattern approximately repeats after three fundamental string periods. A clear sub-twelfth (577 Hz) was audible. Case (b), bowed at a somewhat smaller value of  $\beta$ , shows a less regular but still clearly visible fourth sub-harmonic. In this case, a pitch two octaves below the main note was audible, but less clearly than the sub-twelfth in case (a).

fall on the air resonance of the violin, since the response of that resonance to stray noise can sound somewhat similar.

Fig. 7 shows two examples of velocity waveforms of the string near the bowed point when such sub-harmonics were plainly audible: fairly strong third and fourth sub-harmonics are apparent in Figs. 7a and 7b respectively, the third sub-harmonic being especially clear both aurally and visually. The presence of such sub-harmonics can obviously influence the spread of periods in the jitter measurements described in the previous section, and in that context they were regarded as one of the sources of "spurious" jitter and carefully avoided in the experiments described in section 2. Longer records (not displayed here) showed that the sub-harmonic patterns do not exhibit any long-term regularity, seldom persisting beyond a few sub-harmonic cycles.

As was suggested in the introduction, it turns out that these sub-harmonic phenomena are related to the mechanism of Friedlander's instability of periodic motion in the ideal-string model [9]. The rest of the present section attempts to bring out this relationship and its consequences for understanding real and model string behaviour.

Our approach to the problem of examining this general class of phenomena was suggested by the work of Schelleng [5]. We have extended his ideas somewhat in the effort to make the connection between this work and that of Raman [4] and Fried-

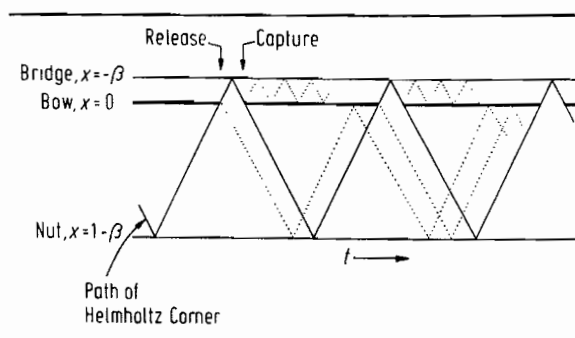


Fig. 8. Window picture, showing the path of the Helmholtz corner in space-time:  $x = (-\beta, 1 - \beta)$  represent the ends of the string, which is of unit length. The heavy line segments at the bowing position,  $x = 0$ , represent the reflecting barriers due to the sticking bow. The gaps in between are the "windows" in space-time, through which disturbances may pass easily since the bow is slipping. The dotted paths correspond to the secondary waves [5], [6], [13] generated in the processes of capture and release of a rounded Helmholtz corner, giving rise to the characteristic pattern of "ripples" in the string velocity waveform noted by Schelleng [5].

lander, as well as continuing his effort to connect theory with observation. The idea that will be useful here, also used by Cremer [13], is that of representing events on the bowed string by means of a space-time (or characteristic) diagram such as that shown in Fig. 8. Distance  $x$  along the string is plotted vertically and time  $t$  horizontally. In the usual Helmholtz motion, the Helmholtz corner or propagating velocity jump traces out the path shown by the solid zig-zag line. The state of the bow-string contact ( $x = 0$  in the diagram) alternates between sticking and slipping, the transitions, "capture" and "release", being triggered by the passage of the Helmholtz corner. In Fig. 8, the heavy lines at  $x = 0$  represent a state of sticking, and the "windows" in between them represent slipping. The term "window" is physically apt because during slipping the bow is almost exactly transparent to any extra disturbance incident upon it, owing to the near-constancy of the coefficient of sliding friction. During sticking the bow acts as a reflecting barrier to small disturbances. In most models neglecting torsional string motion, the reflection is perfect: for the real bowed string it is less so [13].

It is worthwhile to note in passing that Schelleng's beautiful but densely-argued paper [5] on the bowed string is easier to follow with the aid of diagrams like Fig. 8. To take one instance, the fine dotted paths in Fig. 8 are the paths of the "secondary waves" generated at capture and release when the Helmholtz corner is not perfectly sharp [2], [3], [5], [6], [13]. These secondary waves are invoked by

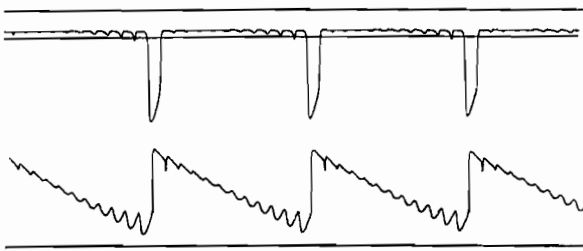


Fig. 9. Computer simulation showing the pattern of Schelleng's ripples at  $x=0$ . Torsional string motion is allowed for, but torsional reflections from the string ends are suppressed for simplicity. The upper trace shows the velocity of the string centre at the bow: the arrival of a secondary wave (cf. dotted lines in Fig. 8) causes the string to roll on the bow. The lower trace shows the corresponding bridge-force waveform. The ripples generated at release are bigger than those generated at capture, because the bow-force is large enough for capture-release hysteresis to operate [2].

Cremer and Lazarus [6] and by Schelleng in his § II J to account for the pattern of "ripples" visible in experimental string-velocity waveforms at the bowed point during the sticking phase of the cycle. A rounded-corner computer simulation [2] which reveals this pattern particularly clearly is shown in Fig. 9.

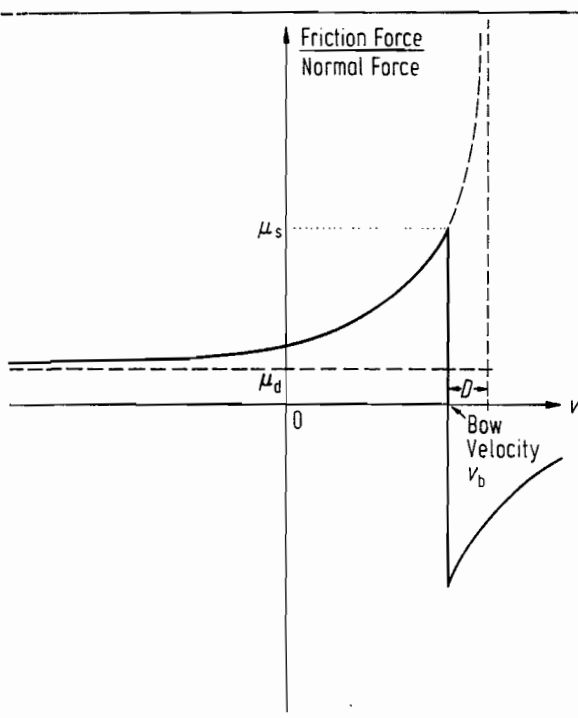


Fig. 10. The friction curve used in all the computer simulations. The slipping portion is a rectangular hyperbola, whose asymptotes are shown dashed. In the simulations  $D=0.2v_b$  where  $v_b$  is bow velocity, and  $\mu_s=1.0$ ,  $\mu_d=0.2$  for qualitative similarity to available experimental data [10].

Now Friedlander's instability involves a rather different class of perturbations to the Helmholtz motion, which can arise even if the Helmholtz corner is perfectly sharp. Consider a small velocity disturbance which goes through any of the windows in Fig. 8, i.e. which impinges on the bow during slipping. To investigate what happens to this disturbance, we first make the usual idealisation that the frictional force  $f(t)$  exerted by the bow on the string depends only on string velocity  $v(t)$  at the bow. Within linearised perturbation theory it is permissible to approximate this dependence simply as

$$f = kv + f_0 \quad (1)$$

where  $k$  and  $f_0$  are constants, since our small disturbance involves only a small segment of the friction curve in the vicinity of the Helmholtz slipping velocity (usually a long way beyond the left-hand edge of Fig. 10). The constant force component  $f_0$  is irrelevant here since it merely imparts a constant, static slope discontinuity to the string at the bowed point. The interest lies in the term  $kv$ . If  $k$  were zero the bow would exert no time-dependent force on the string during slipping, and each window in Fig. 8 would be exactly transparent to small perturbations. However, published measurements of friction curves [10] suggest a shape (like that of Fig. 10) for which  $k$  has a small positive value and thus represents a negative resistance [5] which can slightly amplify the incident disturbance. This turns out to be the basic mechanism of Friedlander's instability: any disturbance is amplified when it passes through a window, and in Friedlander's idealised model there is no compensating dissipation mechanism to attenuate such disturbances.

We now pursue this idea in a little more detail, first verifying the amplification effect then using "window pictures" like Fig. 8 to show that the instability takes the form of a sub-harmonic whose order depends on the value of  $\beta$ . Consider first an ideal, perfectly flexible, lossless string with tension  $T$  and wave speed  $c$ . The general solution for the transverse displacement  $y(x, t)$  associated with a small disturbance may be written in the following well-known form:

$$y(x, t) = \begin{cases} p_1(t - x/c) + q_1(t + x/c), & x < 0 \\ p_2(t + x/c) + q_2(t - x/c), & x > 0 \end{cases} \quad (2)$$

where  $p_i$  and  $q_i$  ( $i=1, 2$ ) are arbitrary functions representing waves travelling respectively towards and away from the bow at  $x=0$ . The corresponding

velocities, i.e. the derivatives of  $p_i$  and  $q_i$  with respect to  $t$ , will be denoted by  $P_i$  and  $Q_i$ . At  $x=0$  we have the jump conditions

$$[y(x, t)]_{x=0-}^{x=0+} = 0 \quad (3a)$$

and

$$T \left[ \frac{\partial y}{\partial x} \right]_{x=0-}^{x=0+} = -k \frac{\partial y}{\partial t} \Big|_{x=0}, \quad (3b)$$

the latter from eq. (1), regarding  $y$  as a perturbation about a state of slipping satisfying eq. (1). Differentiating eq. (3a) with respect to  $t$ , and noting four relations of the type  $-\partial p_1/\partial x = c^{-1}P_1$ , we have

$$\begin{aligned} P_1(t) + Q_1(t) &= P_2(t) + Q_2(t), \\ c^{-1}T[P_1(t) - Q_1(t) + P_2(t) - Q_2(t)] \\ &= -k[P_2(t) + Q_2(t)]. \end{aligned} \quad (4)$$

For convenience we now drop function arguments, and define

$$A = kc/2T = k/2Z \quad (5)$$

as in ref. [2],  $Z = T/c$  being the wave impedance of the string. For simplicity, consider the particular case  $P_2=0$  (i.e. no incoming wave from  $x>0$ ): eqs. (4) then reduce to

$$\begin{aligned} P_1 + Q_1 - Q_2 &= 0, \\ P_1 - Q_1 - (1-2A)Q_2 &= 0 \end{aligned} \quad (6)$$

so that the reflected and transmitted waves are given in terms of the incident wave  $P_1$  by

$$Q_1 = \gamma P_1 \quad (7a)$$

and

$$Q_2 = (1 + \gamma) P_1 \quad (7b)$$

respectively, where

$$\gamma = A/(1 - A). \quad (8)$$

Now  $\gamma$  is finite because the locally stable state of slipping which we are considering must have  $A < 1$  (as mentioned in ref. [5] § II J, and explained further in ref. [2], appendix A); moreover  $\gamma$  is positive because  $A > 0$  for friction curves like Fig. 10. Thus the transmitted wave  $Q_2$  is amplified by the negative resistance at the bow, and there is also a reflected wave  $Q_1$  equal in magnitude to the difference between the transmitted and incident waves. In practice  $\gamma$  tends to be rather small compared with unity.

This result is little changed if we allow for a string with finite torsional wave impedance  $Z'$ , as defined by Schelleng [5], eq. (12). In fact eqs. (7) can be shown to apply as they stand [13], provided that  $\gamma'$

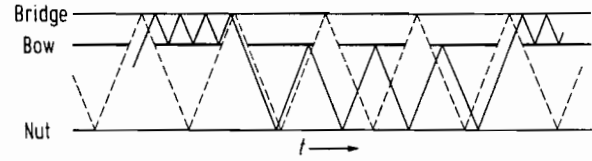


Fig. 11. The path of a sub-harmonic disturbance illustrated in the window picture: in this case, the fourth sub-harmonic is shown. The precisely-timed switching between reflecting and transmitting states represented by the "windows" at  $x=0$  makes the string appear to be exactly four times its actual length, as far as such a disturbance is concerned.

is replaced by

$$\gamma' = \gamma/(1 - \gamma Z/Z'). \quad (9)$$

Also, the amplitude of the torsional wave generated is  $Z/Z'$  times that of the reflected transverse wave given by the modified eq. (7a). It can again be shown that local stability of the slipping state implies that  $\gamma'$  is finite and positive, and moreover that  $\gamma' > \gamma$ . Thus the torsional degree of freedom, far from inhibiting the amplification mechanism for transverse waves, actually enhances it somewhat — essentially by increasing the ratio  $A'$  of negative resistance  $k$  to total radiation resistance  $2(Z^{-1} + Z'^{-1})^{-1}$ . We recall that Schelleng's measured values of  $Z/Z'$  lie between 0.26 and 1.

We now consider the path in the window picture of a small transverse wave which passes through a window. It is not hard to see by geometrical construction that such paths are always periodic, and that their periods are integral multiples of the period of the Helmholtz wave. An example is given in Fig. 11, showing a period four times the Helmholtz period, that is to say a fourth sub-harmonic. This periodicity implies that the amplification due to transmission through windows is repeated indefinitely as time goes on. This not only explains the exponential instability of the Helmholtz motion in an ideal string discovered by Friedlander, but also shows that it will always take the form of a sub-harmonic.

In addition we can now see why Friedlander was able to stabilise the motion either by choosing a friction curve such that  $k \leq 0$  (see also Keller [14]), or by introducing dissipation at the bow: obviously any kind of dissipation will do, as long as its net effect over the sub-harmonic cycle is at least large enough to balance the net amplifying effect of the negative resistance at each window. The Raman model [2], [3], [4] can thus achieve a similar stabilisation of the Helmholtz motion, since although it involves an ideal string there are resistive terminations at the ends.

To check these ideas, a complete analysis based on eqs. (7) has been carried out for the Raman mod-

el. It involves keeping track of all the reflections at windows implied by eq. (7a), as well as the transmissions governed by eq. (7b), and therefore consideration of a set of interlocking sub-harmonic paths all of the same order. We omit the details (which it is hoped to publish elsewhere) but remark that such an analysis does indeed give precise agreement with the exponential growth-rates and stability thresholds predicted by Friedlander's original method and its extension to the Raman model. This has been checked both by analytical calculation and by numerical experiments using the computer implementation of the Raman model.

It is of interest to know which orders of sub-harmonics are accessible for a given bow position. The window picture reduces this to a purely geometrical problem, to which the answer is easily found to be that the  $N$ th sub-harmonic is possible for values of  $\beta$  anywhere between

$$1/(N-1) \quad \text{and} \quad 1/(N+1).$$

Thus a fourth sub-harmonic like that shown in Fig. 11 is possible for  $1/3 > \beta > 1/5$ . Conversely, for a given non-integer  $\beta^{-1}$  two sub-harmonics are possible, whose periods in units of the fundamental string period are the two integers nearest to  $1/\beta$ .

We now return from idealised models to the observed sub-harmonics in real strings. It is plain that the insight given by the window picture is still rele-

vant, and we suggest that the existence of sub-harmonic paths explains the sub-harmonic behaviour seen in Fig. 7. This explanation is indeed consistent with the observed dependence of sub-harmonic order on  $\beta$ . However for real strings the threshold for self-excited sub-harmonics is very different from that in simple models without torsional string motion. The threshold is determined by the net loss along the appropriate set of sub-harmonic paths, which must be balanced by the net effect of negative resistance. For real strings the principal loss is due to coupling to torsional waves at the sticking bow. Cremer [13] shows that for realistic values of string parameters this loss (as measured by the reflection coefficient for transverse wave amplitude) is typically of order 30%. (This figure is to be compared with the 1% or less typical of absorption coefficients at the ends of the string.) This means that while Friedlander's instability tends to be ubiquitous in models neglecting torsional motion, it is hardly likely to be observed in real string motion. What we do observe in the experiments typified by Fig. 7 is presumably the effect of transient disturbances dying away along sub-harmonic paths, rather than the growth of self-excited disturbances. Irregularities in rosin distribution on the bow-hair appear to be sufficient to generate such sub-harmonic disturbances. If in place of a bow a rigid, rosined stick is used (as described previously [2]), these irregularities are greater, and sub-harmonics are then more apparent to the ear: indeed, it was when experimenting with such a stick that we first became aware of the existence of audible sub-harmonics.

Another observable consequence of the sub-harmonic mechanism is illustrated in the two bridge-force waveforms of Fig. 12. The top waveform is an observed one, obtained with the stick on a thin metal string on the monochord, and a rather large bow-force to maximise  $k$  and therefore the persistence of sub-harmonic disturbances. This is to be compared with the second waveform, a Raman model simulation. The feature shared by the two is the approximate regularity of the pattern which makes up the band of "fur" occupying each cycle, which contrasts with the variation of this pattern from cycle to cycle. During each cycle we are seeing a "window-full" of some disturbance trapped in the short end of the string and reflecting back and forth as suggested in the top left of Fig. 11. This disturbance then escapes during slipping, while a new window-full (not indicated in Fig. 11) is admitted. In the simulation the waveform of the disturbance is very regular, while in the observed waveform the shape changes slightly after each

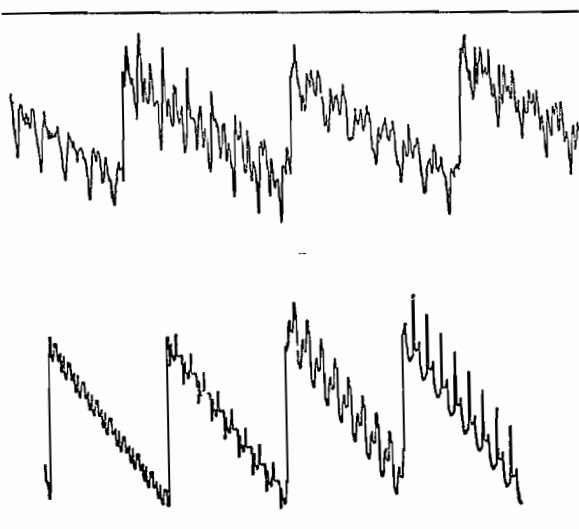


Fig. 12. Sub-harmonic "fur" patterns in bridge-force waveforms. Top trace shows observed bridge force from bowing a metal string (0.007 inch diameter rocket wire) on a monochord with the rosined stick (see text). Bowing conditions are roughly as for Fig. 2, except that bow-force is much larger. Lower trace shows a Raman-model simulation of a similar phenomenon.  $\beta \cong 1/7$  and  $1/9$  respectively in the two cases.

reflection as would be expected with a real string and bridge.

To summarise the main results of this section, then, the sub-harmonic paths made evident by window pictures like Fig. 11 are the key to understanding some types of departure from periodic Helmholtz motion — both in real strings and in idealised theoretical models. However, for real strings the sub-harmonic mechanism seems to be only of minor importance, except perhaps under highly transient conditions.

#### 4. Spikes

##### 4.1. Experimental evidence and proposed explanation

There thus remains the problem of the audible noise in loud playing of a musical note with the bow near the bridge, which is of direct concern to the musician but which has turned out to be unconnected with the types of aperiodicity discussed up to now. A clue to the source of the audible noise is readily found on examination of the bridge-force waveform during the playing of such noisy notes. A typical example is shown in Fig. 13a, where an open violin *G* string is played with an ordinary bow in such a way as to produce the noise at a moderate but plainly audible level. Although we mentioned in section 2 that the timing of the Helmholtz fly-back does not show great cycle-to-cycle variation even in such cases, it is plain that the waveforms

do show considerable aperiodicity, largely in the form of sharp spikes superimposed on the Helmholtz sawtooth. We have found from many observations that such spikes always appear when the noise builds up. A more extreme example, taken at larger bow-force, is shown in Fig. 13b. This shows fewer, larger spikes and corresponds to a noise level too high for extensive use in most musical circumstances, even though the musical pitch is still quite stable. If the bow-force is increased still further the musical note is finally lost, giving way to a "raucous" vibration regime when the Helmholtz corner can no longer release the bow from sticking [5].

The fact that the time-separation and amplitude of the spikes is sensitive to bow-force distinguishes them unequivocally from two other types of observable deviation from an ideal sawtooth waveform, with which they might at first sight be confused. The experimental bridge-force waveform in Fig. 14a, for  $\beta$  very near  $1/4$ , illustrates both types but shows no spikes. The first of these deviations arises from the secondary waves generated during the processes of capture and release by a rounded Helmholtz corner and giving rise to "ripples" in the waveform as already mentioned in connection with Figs. 8 and 9. The second deviation from a sawtooth, strongly in evidence in Fig. 14a, arises from the tendency of any harmonics having nodes sufficiently close to the bowed point to be greatly reduced in amplitude, giving rise to the "crumples" in the waveform first noted by Helmholtz [15]. Un-

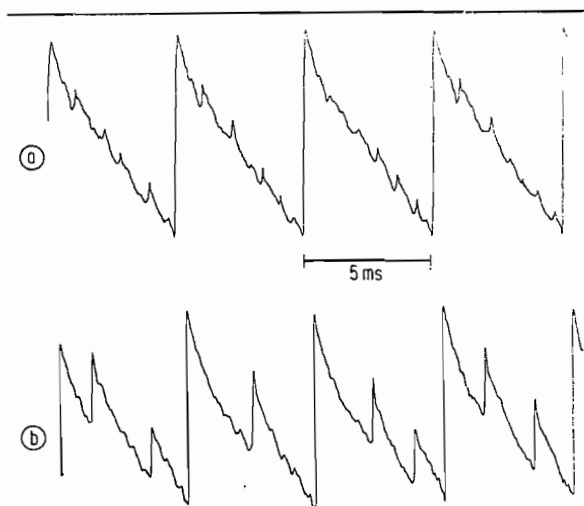


Fig. 13. "Spikes" in bridge-force waveforms obtained by hand bowing with a normal bow on the open *G* string of a violin. The inner edge of the bow-hair was about two-thirds of a bow-width from the bridge. Upper trace is for lower bow force, lower trace for higher bow force at approximately the same distance from the bridge.

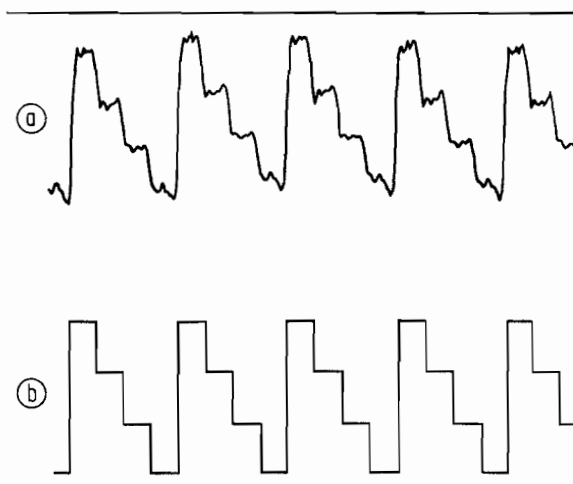


Fig. 14. (a) Ripples and Helmholtz "crumples" observed in the bridge-force waveform for the open *G* string of a violin bowed with a normal bow with  $\beta = 1/4$ ; (b) the crumples as predicted by the Raman model in the same situation, in the limit of small dissipation. (The four-step "staircase" arises from the absence of the 4th, 8th, 12th etc. harmonics of an ideal sawtooth wave; e.g. [3].)

like secondary waves, crumples do not depend on corner-rounding and occur even in the Raman ideal-string model as illustrated in Fig. 14 b, which shows the Raman-model idealisation corresponding to Fig. 14 a. Both ripples and Helmholtz crumples produce patterns within each Helmholtz cycle which roughly speaking repeat with periods of  $\beta$  times the Helmholtz period, for all values of bow-force in the usual range. This useful diagnostic feature is sufficient in itself to distinguish them from spikes, whose time-separation bears no unique relation to  $\beta$ , as well as tending to be irregular.

Our proposed explanation for spikes is that they originate in the finite width of the ribbon of bow-hair in contact with the string, and that the mechanism which produces the spikes is differential slipping, in which some but not all of the bow-hairs release from time to time during the nominal "sticking" phase of the Helmholtz cycle. This hypothesis can immediately be seen to be consistent with several general features of observed spike behaviour. First, spikes are most easily produced with the bow near the bridge. Since the variation of  $\beta$  across the width of the bow is then very large, it is reasonable that an effect of finite bow-width should be strong. Second, the very aperiodicity and suddenness of the spikes suggests a mechanism connected intimately with the stick-slip nonlinearity of the bow-string contact, just as for the main flyback. Lastly, and most telling, we have never succeeded in producing spikes with the rosined stick described earlier [1], [2], which has only a very small width of contact with the string.

To test the proposal, a "double stick" was made from a length of wooden dowel similar to that used for the stick described earlier. A groove was cut along its length, giving it the cross-section shown in Fig. 15. The two parallel edges of this groove

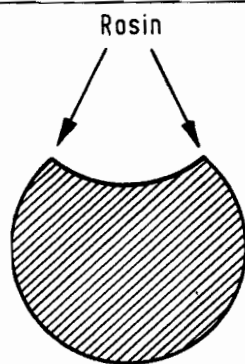


Fig. 15. The cross-section of the "double stick". The distance between the two rosined edges which contact the string is about 5.5 mm.

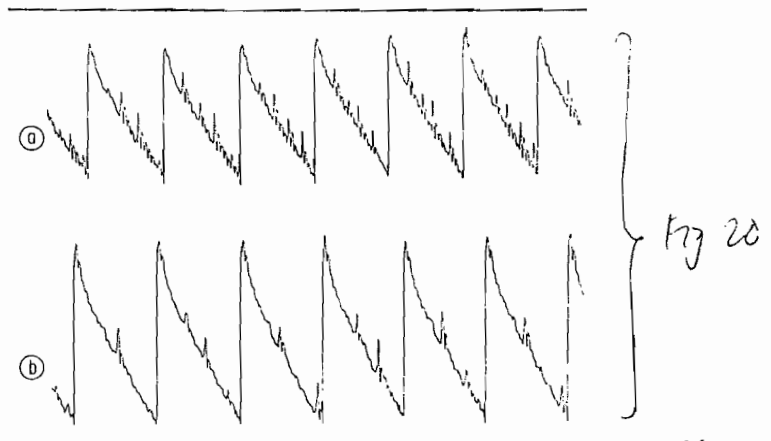


Fig. 16. Spikes in bridge-force waveforms obtained with the double stick at about the same position on the string as was the bow in Fig. 13 (Compare also with Figs. 18 d, e).

were smoothed and rosined, and the double stick used to bow the string, with both edges in contact. This immediately produced spikes similar to those made by the bow, albeit more regular: two examples are shown in Fig. 16 under similar bowing conditions to the waveforms of Fig. 13. This is very compelling evidence for the general correctness of the differential-slipping hypothesis, which should of course apply perfectly well to two separated "bow-hairs" if it applies at all.

The proposed mechanism, when elaborated in more detail, can moreover explain the observed dependence of the time-separation and amplitude of spikes upon bow-force. The next sub-section is devoted to showing this by means of simple theoretical arguments together with appropriate computer simulations; see also section 5.

#### 4.2. Theory and discussion

For theoretical purposes it is of course easier to model the double stick with two "hairs" than a real bow with many hairs. Suppose tentatively that a Helmholtz-like motion occurs (as in the experiments) and that at the beginning of the nominal sticking phase of the Helmholtz cycle the string is in the position marked "1" in Fig. 17 a. String displacements are assumed small, but are drawn exaggerated; only the end of the string nearest to the two bow-hairs is shown. In position 1, the Helmholtz corner has just propagated past the bow from left to right. While the string sticks to both hairs, the short section of string between the hairs is carried forward parallel to its initial position, leading to the situation shown as position 2 in the figure.

We now ask how far through the nominal sticking period of the Helmholtz motion this situation can

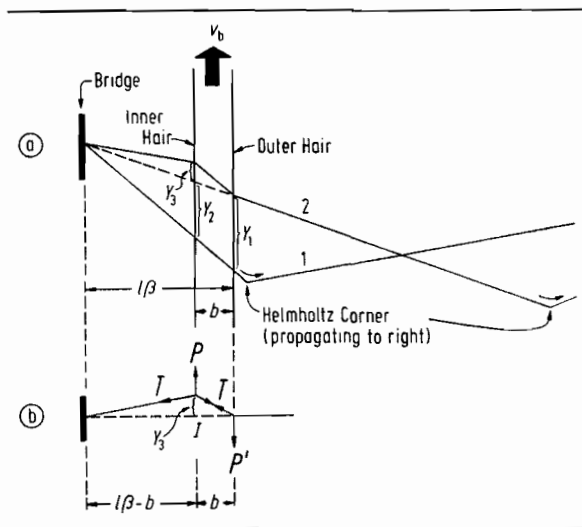


Fig. 17. (a) Hypothetical string positions if sticking persists at both bowing points during a fraction of the Helmholtz sticking phase. Position 1 is the hypothesised string position just after outer-hair capture, and position 2 is the string position later in the sticking phase. The DC component of the friction force, and corresponding kinks in the string at the bow hairs in position 1, are unimportant for the argument and are ignored for simplicity.

(b) The configuration of position 2 with a constant slope subtracted out.

persist. The friction required at the inner hair to sustain position 2 cannot be significantly less than the value given by simple statics, since any stray disturbances trapped in the two short sections of string between bridge and bow hairs will tend to promote rather than inhibit the onset of slipping. The static value  $P$  of the required friction force, for small string displacement, is simply

$$P = -T \left[ \frac{\partial y}{\partial x} \right]_-^+ = T \left( \frac{Y_3}{l\beta - b} + \frac{Y_3}{b} \right) \quad (10)$$

in the notation of the figure,  $T$  being the tension in the string and  $l$  the string length;  $\beta$  now refers to the position on the string of the outer hair. (The expression on the right-hand side is most easily verified by inspection of Fig. 17b, which gives the string shape for position 2 with a constant slope  $\partial y/\partial x$  subtracted out, a procedure which clearly leaves the middle expression in eq. (10) unchanged.) From Fig. 17a,  $Y_2/Y_1 = (l\beta - b)/l\beta$ , so that

$$Y_3 = Y_1 - Y_2 = Y_1 \delta, \quad (11)$$

where  $\delta = b/l\beta < 1$ , the position of the inner hair as a proportion of the short string length. As  $Y_1$  and therefore  $Y_3$  increase with time during the sticking phase,  $P$  increases also. Slipping must have occurred by the time  $P$  reaches a value

$$P_s = \mu_s F_I,$$

if not earlier, where  $\mu_s$  is the coefficient of static friction, typically of order unity, and  $F_I$  is the normal bow-force on the inner hair. The corresponding value of  $Y_1$ , say  $Y_{1s}$ , is obtained by substituting  $P = \mu_s F_I$  into eq. (10) and using eq. (11); the result is

$$Y_{1s} = \frac{\mu_s F_I}{T} l\beta(1 - \delta). \quad (12)$$

Now  $Y_{1s}$  is usually much less than the total displacement  $Y_{1H}$  for the whole of the sticking phase of the Helmholtz motion, as will be verified shortly; therefore slipping will usually occur during the nominal sticking phase. Moreover it will tend to occur at the inner hair, since it is evident from Fig. 17b that the static force  $P'$  at the outer hair is somewhat smaller in magnitude than  $P$ .

Computer simulations confirming these ideas for the case  $\beta = 0.036$ ,  $\delta = 1/2$  over the usual tolerance range of normal bow forces  $F_b$  are shown in Fig. 18. The model used is a two-bowing-point version of the model described in § 5 of ref. [2], in which rounding of the Helmholtz corner by real-string effects is allowed for, except between the two bowing points where it is assumed to be negligible. Bow-force increases from top left to bottom right of Fig. 18, from the case (a), near Raman's minimum bow-force, where the Helmholtz motion is about to give way to a double-slip motion (at twice the string's natural frequency) to case (f), near Schelleng's maximum bow-force, where the motion is about to undergo catastrophic breakdown to a raucous regime. The upper trace of each set of three shows transverse force on the bridge, and cases (d) and (e) are qualitatively comparable with the experimental waveforms of Figs. 16a and 16b. The middle and lower traces in each set show string velocity at the inner and outer bowing points. As expected, differential slipping does occur at the inner hair; and the spike-like jumps in the bridge-force waveforms are clearly in one-to-one correspondence with the differential slipping events.

The argument leading to eq. (12) suggests that for a given bow speed and position, both the time separation and amplitude of the spikes should increase with  $Y_{1s}$  and therefore with increasing bow-force. This is just what is observed in Fig. 18, as well as in the laboratory experiments typified by Figs. 13 and 16. For low bow-forces the inner hair slips many times per cycle: indeed in case (a) of Fig. 18 it never sticks. Then as force is increased the differential slipping events become less frequent but more violent. A more quantitative estimate of the relation between bow-force and the time separation and amplitude of spikes will be given in the next

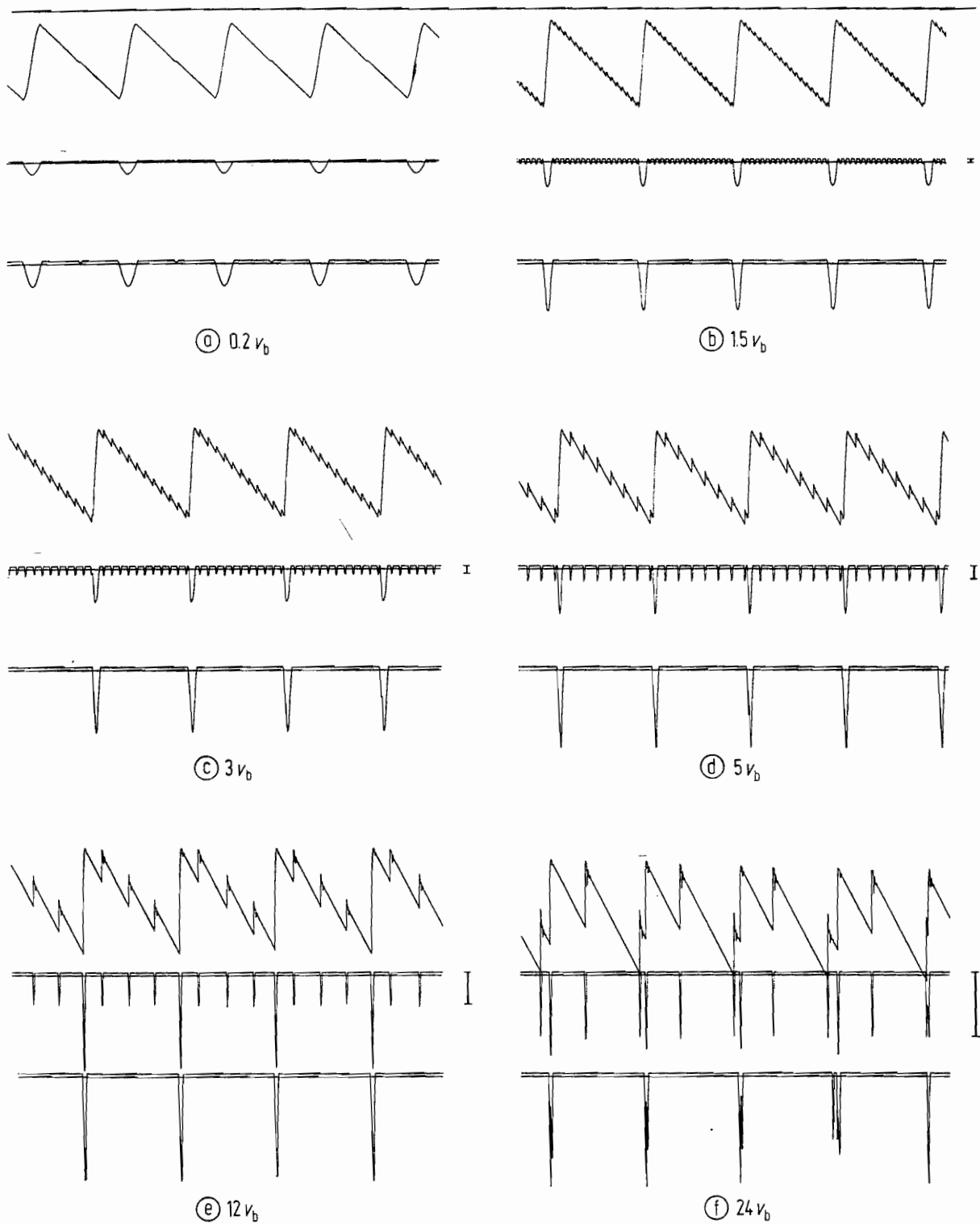


Fig. 18. Simulated waveforms from the two-bowing-point, rounded-corner model, using the friction curve of Fig. 10. In each case, the top trace shows transverse force on the bridge, the second trace the string velocity at the inner bowing point, and the lower trace the string velocity at the outer bowing point. The two bowing points divide the string in the ratios 2 : 2 : 107, so that  $\beta = 4/111 \cong 0.036$  and  $\delta = 0.5$ . The force on each bow-hair is given beneath the pictures, in units for which the characteristic impedance  $Z = T/c$  of the string is  $1/2$ . Equal forces on the two hairs were maintained throughout. For orientation, eq. (14) gives Schelleng's maximum bow-force for the outer hair as  $34.7v_b$ . Corner-rounding of waves reflected from either string termination is achieved by convolution of outgoing waves with an arbitrary "corner-rounding function", here taken for simplicity as a Gaussian  $\exp\{-(t-t_r)^2/1.5\}$ ,  $t$  being in time-step units (222 per fundamental period), and  $t_r$  being the delay for reflection. There is no corner-rounding of waves travelling between the two bowing points. The vertical bars on the right give the minimum differential-slipping velocity as predicted by eq. (17) below.

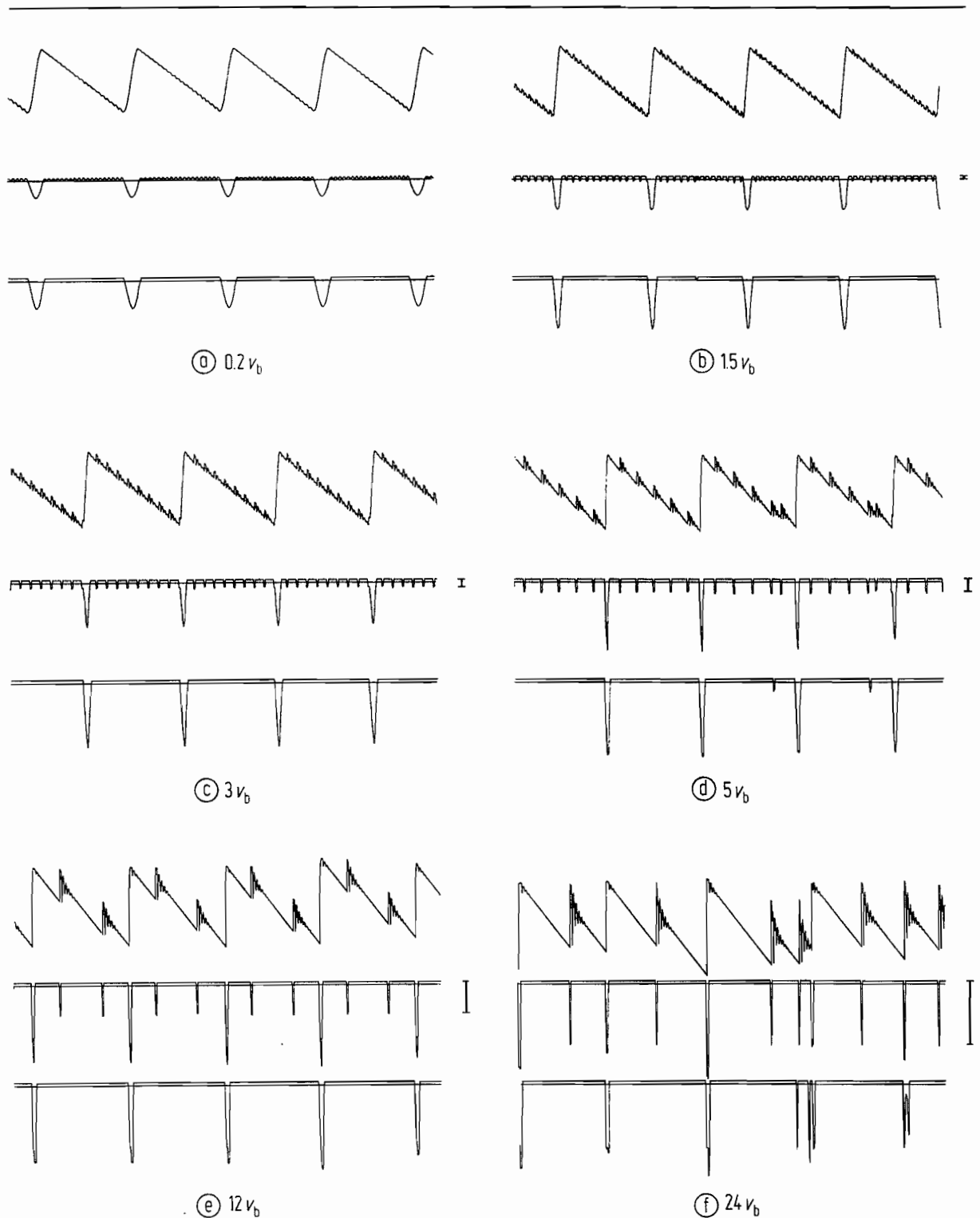


Fig. 19. Simulated spikes from the two-bowing-point, rounded-corner model, with parameters the same as in Fig. 18 except that the two bowing points divide the string in the ratios 3 : 2 : 107 here ( $\beta = 5/112 \cong 0.045$ ;  $\delta = 0.4$ ). The plotting scales and relative vertical displacements of the traces are all equal, and the same as those of Fig. 18. Schelleng's maximum bow force from eq. (14) is  $28v_b$ .

section, where the use of this relation to probe friction characteristics experimentally is discussed.

We can now verify that the quantity  $Y_{1s}$  of eq. (12) is indeed small compared to the total string displacement  $Y_{1H}$  under most circumstances of interest. Since the Helmholtz-like motion exhibited in Fig. 18 is controlled mainly by the outer hair, we may estimate the order of magnitude of  $Y_{1H}$  in terms of the bow speed  $v_b$  and the wave speed  $c$  on the string as

$$Y_{1H} = v_b 2l(1 - \beta)/c, \quad (13)$$

i. e. just as for the ideal Helmholtz motion with the inner hair absent. The maximum bow force on the outer hair for which the Helmholtz motion is possible may be roughly estimated by Schelleng's formula

$$F_{\max} = 2T v_b/\beta c(\mu_s - \mu_d) \quad (14)$$

([5], eq. (2) and footnote 10), where  $\mu_d$  is the dynamic coefficient of friction corresponding to a relative slipping velocity  $v_b/\beta$ . Combining eqs. (12), (13) and (14) and ignoring a factor  $\mu_s/(\mu_s - \mu_d)$ , which is typically of order unity, we get

$$\frac{Y_{1s}}{Y_{1H}} \cong \left( \frac{F_I}{F_{\max}} \right) \left( \frac{1 - \delta}{1 - \beta} \right). \quad (15)$$

In modern violin playing the effective value of  $\delta$  can easily approach unity, and when  $\delta$  is not large, i. e. when not playing close to the bridge,  $F_I$  seldom exceeds a small fraction of  $F_{\max}$ . Hence  $Y_{1s}/Y_{1H}$  will be substantially less than unity under most circumstances of interest, so that differential slipping must be expected to occur as a rule.

It remains to discuss the question of when differential slipping should occur irregularly, and hence give rise to an audible impression of noise in addition to the steady note. Accordingly we take a closer look at the dynamics of the short end of the string considered in isolation during the time the outer hair sticks. The problem is equivalent to that suggested by Fig. 17b and eq. (11), in which the short end of the string has fixed terminations and the inner hair moves with reduced speed  $v_b \delta$ . We can now apply eq. (14) to get the Schelleng maximum bow-force  $F_{I\max}$  for the isolated short end, by using  $v_b \delta$  in place of  $v_b$ , and  $\delta$  in place of  $\beta$ . This gives  $F_{I\max} = \beta F_{\max}$ , neglecting the somewhat different value of  $\mu_d$  appropriate to the smaller relative slipping velocity involved. This result should be taken only in an order-of-magnitude sense, if only because Schelleng's approximations are not appropriate unless  $\delta \ll 1$ ; nevertheless the fact that for small  $\beta$ ,  $F_I$  will often exceed  $F_{I\max}$  while remaining well below  $F_{\max}$  suggests that the short

end will often vibrate in a raucous regime [5]. But the essential character of the raucous regime is that it has no time-keeping device as powerful as the Helmholtz corner, so that the timing of differential slips will be much more sensitive to external irregularities than is the main Helmholtz slip. This well explains why audible noise, associated with differential slipping at the inner hair, can coexist with a musical note, maintained by the Helmholtz timekeeping mechanism on the whole string. Our picture also suggests that only for the smaller bow-forces in the usual tolerance range can we expect differential slipping to be regular in practice. Experimentally, the characteristic symptoms of spikes do indeed tend to disappear, as does the audible noise, as bow-force is decreased. At extremely low bow-forces, some of the bow-hairs of a real horsehair bow presumably never stick, as is suggested by Fig. 18a.

In confirmation of our diagnosis of the origin of irregularity in spike-timing, it will be noted that the observed waveforms of Figs. 13 and 16 show spikes that are more irregular than those in the simulated waveforms in Fig. 18. Any externally-imposed irregularity in the simulation (arising from numerical errors) will be much less than that occurring in practice with either real bows or real sticks. This is further supported by numerical experiments (omitted for brevity) in which irregularity was deliberately introduced into the model in the same way as described at the end of section 2: the simulated spikes did, then, become much more irregular.

In Fig. 19, we show some more simulated waveforms, this time for  $\delta = 0.4$ , i. e. with the two bowing points moved a little further from the bridge to separate more clearly the first spikes caused by the

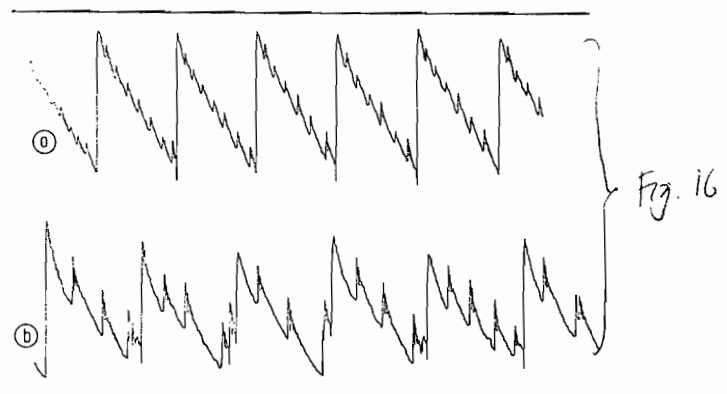


Fig. 20. Observed spikes in bridge-force waveforms, (a) using the double stick at  $\delta \cong 1/3$ ; and (b) using a normal bow at about the same position on the string. Other bowing conditions were similar to those used for Figs. 13a and 16a.

differential slips from the chains of reflections which follow. The width of the differential-slip pulses of each middle trace of Figs. 19b–f is given precisely by the travel time  $2l\beta\delta/c$  for a velocity pulse from the inner hair to the outer (sticking) hair and back. The arrival back at the inner hair of the inverted reflection of the pulse sent out on release apparently causes recapture at the inner hair. The subsequent reflections take place mainly in the longer section of string between inner hair and bridge, as is evident from the time between successive spikes in each chain of reflections in the bridge-force waveforms, which is found to be equal to  $2l\beta(1-\delta)/c$ . Fig. 20 shows two roughly comparable experimental waveforms; waveform (a) is from the double stick with  $\delta$  close to  $1/3$ , and waveform (b) is from a real bow in a similar position.

#### 4.3. Concerning the Saunders loudness test

Our observations of spikes raise a question concerning the Saunders "loudness test" [16] in which sound-pressure-level readings are taken when an instrument is bowed "as loudly as possible". Unfortunately the threshold for this does not seem clearly defined in an objective way. For a given bow speed, loudness (or at least amplitude of the Helmholtz motion) increases as  $\beta$  is decreased; but how small  $\beta$  can be made is limited in practice by the build-up of the noise associated with spikes. Thus how loudly one can play depends on just how noisy a note one is prepared to tolerate. The good repeatability of loudness tests developed by those who are well practised at them thus appears to depend on consistent judgement of audible noise level as well as bow speed.

### 5. Spikes and related phenomena as an experimental probe of friction characteristics

It is clear from the discussion given in refs. [2] and [3] that in any detailed comparison of computer simulations with observed string motion, an important input to the simulation must be the shape of the friction curve. For that matter, the assumption of a single friction curve as in Fig. 10, made in our current models and in all earlier work, is itself an idealisation which ought to be tested. It presumes that friction force depends only on the instantaneous relative velocity of the sliding surfaces and not on the history of the relative motion. Measurements of friction curves for rosin [10] have hitherto been made only during nominally steady relative motion of the surfaces, and then not using horsehair. It is therefore far from clear to what extent a friction curve, so measured, is relevant to

the real bowed string with very short-time-scale changes in relative velocity taking place: as we have suggested before [2], a more complicated rosin tribology might be appropriate. To resolve such questions it is desirable to find ways of measuring the frictional behaviour of the bow-string contact while the string is vibrating. In this section we indicate briefly how observations of spikes and related phenomena can provide some of the needed information in a simple way.

Considering again the problem for the isolated short end of the string suggested by Fig. 17b, we can estimate the size of the velocity jump when the inner hair releases as follows. We again assume simple statics up to the moment of release when the friction force  $P$  reaches the value  $P_s = \mu_s F_I$ . Then events immediately after release are given by the standard solution to the plucked-string problem [17], with modifications to allow for the facts that (i) each point of the string is moving with a constant speed just before release, the speed at the inner hair I being  $v_b \delta$ , and (ii) the force  $P$  does not jump to zero as in the pluck problem but, rather, jumps by an amount  $\Delta P$  down to the value appropriate to slipping friction. The corresponding slip velocity is determined by the jump  $\Delta v_I$  in the velocity  $v_I$  of the string at the inner hair I in Fig. 17b. It follows from the standard theory that

$$\Delta v_I = \Delta P / 2Z, \quad (16)$$

where  $Z = T/c$  is the wave impedance of the string as before: this is because each section of the string presents a radiation resistance  $Z$  to whatever transverse force is exerted on it. Therefore if the friction-curve idealisation holds,  $\Delta v_I$  is determined by the geometrical construction shown in Fig. 21. A

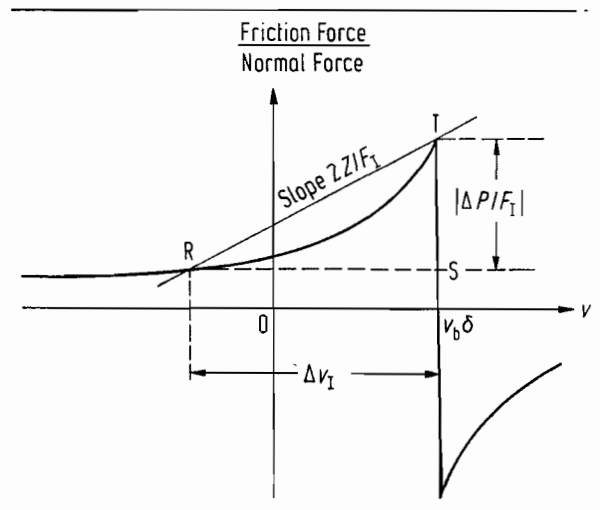


Fig. 21. Graphical construction for  $\Delta v_I$  (see text).

straight line of slope  $2Z/F_I$  is drawn through the tip  $T$  of the friction curve; the magnitude  $\Delta v_I$  is given by  $RS$ , where  $R$  is the intersection of the left-hand "slipping" portion of the friction curve with the straight line. (This is nothing but a special case of the Friedlander-Keller graphical construction whose dynamical implications were discussed at length in ref. [2].) For the case of the hyperbolic friction curve of Fig. 10, it is readily shown that

$$\Delta v_I = \max [0, (\mu_s - \mu_d) (F_I/2Z) - D]; \quad (17)$$

$\Delta v_I$  is zero when  $F_I$  is smaller than the value  $F_{crit}$  for which  $R$  coincides with  $T$ . Values of  $\Delta v_I$  calculated from eq. (17), with  $\mu_s - \mu_d = 0.8$  and  $D = 0.2v_b$ , are indicated graphically by the vertical bars at the right of each inner-hair waveform in Figs. 18 and 19 (except in Figs. 18a and 19a, for which  $\Delta v_I = 0$ ). Many of the actual velocity jumps in the inner-hair waveforms slightly exceed  $\Delta v_I$ , as would be expected from the fact that release will usually be assisted by stray disturbances neglected in the argument above. However the smallest of the jumps observed over a few dozen differential slipping events appears to give a good estimate for  $\Delta v_I$ ; and therefore observations of  $\Delta v_I$  over a range of inner-hair forces  $F_I$  in a double-stick experiment in which  $F_I$  is adequately controlled, should supply information about the friction characteristics during release. In practice the effect of torsional string motion would have to be allowed for, but this is straightforward using the ideas of [5] or [13]: the result is that the sloping line in Fig. 21 now has slope  $2ZZ'/F_I(Z+Z')$ , in the notation of eq. (9), with  $\Delta v_I$  now representing the jump in velocity at the surface of the string. The jump in velocity at the centre is a factor  $Z'/(Z+Z')$  less.

The time  $\tau$  between differential slips also contains information about  $\Delta v_I$  and therefore about friction characteristics during release. Assuming that recapture occurs at the return of the first reflection from inner hair or bridge, i.e. after a time  $2l\beta c^{-1} \min(\delta, 1 - \delta)$ , we can estimate the backwards displacement at  $I$  of the short end of the string during slipping as

$$2\Delta v_I l \beta c^{-1} \min(\delta, 1 - \delta), \quad (18)$$

as in the standard pluck problem, if we neglect the contribution to the net displacement due to the initial string velocity distribution<sup>1</sup>. The time be-

<sup>1</sup> The correction, expressed as a fraction of  $\tau$  as given by formula (19), is  $-v_b/\Delta v_I$  times

$$\varepsilon(1 - 2\varepsilon)/(1 + 2\varepsilon) \leq 1.5 - \sqrt{2} < 0.09$$

for  $0 \leq \delta \leq 1$ , where  $\varepsilon = |0.5 - \delta|$ . Since  $v_b/\Delta v_I$  is typically well below unity, the correction only slightly shortens  $\tau$ , and indeed vanishes for  $\delta = 0, 0.5$ , or  $1$ .

tween slips is the time taken for the displacement to be made good by the sticking string moving at the effective bow speed  $v_b \delta$  (again recall Fig. 17b), namely

$$\tau \cong \frac{2l\beta}{c} \frac{\Delta v_I}{v_b} \left[ \frac{\min(\delta, 1 - \delta)}{\delta} \right]. \quad (19)$$

Despite the approximations we have made, this expression agrees to ten percent or so with the sticking times between differential slips in Figs. 18c and d and in Figs. 19c, d and e, except in those comparatively rare instances when the assumption of a sticking outer hair is violated as in Fig. 19d. The longest time between differential slips in Fig. 18e is about ten percent shorter than the estimate (19). It should be noticed incidentally that  $\tau$  expressed as a fraction of the fundamental period  $2l/c$  is roughly comparable, for small  $\beta$ , with the more naive order-of-magnitude estimate suggested by eq. (15). To show this, refer to eqs. (14) and (16) and use the facts that  $\Delta P$  is of the order  $(\mu_s - \mu_d) F_I$  and that the expression in square brackets in eq. (19) is always within a factor 2 of  $(1 - \delta)$ , for  $0 \leq \delta \leq 1$ . For quantitative purposes, however, the expression (15) tends to underestimate  $\tau/(2l/c)$  somewhat, a factor of up to 2 arising because the backwards displacement of the short section of the string during slipping takes it beyond its equilibrium position before recapture, a fact taken account of in eq. (19) but not in eq. (15).

For a quantitative experiment it may prove to be best to use the raucous regime of vibration in isolation, i.e. simply to set up the conditions suggested by Fig. 17b alone. In practice one would work with a greater length of string so that an ordinary bow could be applied effectively at one point only. It may also prove best to observe the first slip when the bow or stick is started slowly from rest, since the conditions envisaged in our derivation of eqs. (16) and (19) would then be realised more accurately. A closer analysis of this situation, taking into account the velocity distribution on the string at first release, torsional motion, and string terminations with variable reflection coefficients, suggests the possibility of measuring the capture behaviour as well as the release behaviour. There is of course no guarantee that capture behaviour for a real bow is given by the same friction characteristic as release behaviour, and so direct experimental information on capture behaviour is highly desirable.

## 6. Conclusion

We have examined three ways in which the motion of a bowed string can depart from a regular

Helmholtz motion. We have seen that the time-keeping of the Helmholtz corner itself, and therefore of the main flyback in the bridge-force waveform, does not exhibit great variation — in fact considerably less than previously reported. Such variations as were observed seem attributable merely to irregularities in rosin distribution or other factors not intrinsic to the basic dynamics. However the waveform of the motion can exhibit essentially two other kinds of departure from strict periodicity, sub-harmonics and spikes, either of which can coexist with regularly-spaced Helmholtz flybacks. Spikes (e.g. Fig. 13) can produce a major audible effect, and set obvious limits on the bowing parameters used by musicians.

In each case considered, we have been able to find a likely cause for the observed effect, and we have given computer simulations to confirm this, in considerable detail in the case of spikes. As an unexpected bonus, our attention has been drawn to possible methods for measuring frictional characteristics under real playing conditions. Such measurements could make an important contribution toward bridging the large gap still remaining between observations and quantitative theories of bowed-string motion.

#### Acknowledgements

The authors are indebted to Prof. L. Cremer for some penetrating comments on the first version of this paper. J. W. thanks Clare College, Cambridge for financial support, and R. T. S. thanks Carnegie-Mellon University for the sabbatical support in the spring semester of 1977 which made this collaboration possible. The Cambridge University Engineering Department generously provided computing and laboratory facilities. Samples of rocket wire were kindly supplied by the Super Sensitive Musical String Co., of Sarasota, Florida.

(Received October 15<sup>th</sup>, 1979.)

#### References

- [1] McIntyre, M. E. and Woodhouse, J., The acoustics of stringed musical instruments. *Interdisciplinary Sci. Rev.* **3** [1978], 157. This reference gives a fairly extensive bibliography of earlier work.
- [2] McIntyre, M. E. and Woodhouse, J., On the fundamentals of bowed string dynamics. *Acustica* **43** [1979], 93.
- [3] Schumacher, R. T., Self-sustained oscillations of the bowed string. *Acustica* **43** [1979], 109.
- [4] Raman, C. V., On the mechanical theory of vibrations of bowed strings. *Ind. Assoc. Cult. Sci. Bull.* **15** [1918], 1.
- [5] Schelleng, J. C., The bowed string and the player. *J. Acoust. Soc. Amer.* **53**<sup>1</sup> [1973], 26. Schelleng's main results on bowing tolerance are given in his eqs. (1a) and (2), and in his footnote 10.
- [6] Cremer, L. and Lazarus, H., Proceedings of the 6th International Congress of Acoustics, Tokyo 1968 N. 2—3. See also Cremer, L., Der Einfluss des "Bogendrucks" auf die selbsterregten Schwingungen der gestrichenen Saite. *Acustica* **30** [1974], 119; an English translation of an earlier version appears in *Catgut Acoust. Soc. Newsl.* **18**<sup>1</sup> [1972], 13 and **19**<sup>1</sup> [1973], 21.
- [7] Cardozo, B. L. and Van Noorden, L. P. A. S., 3rd Ann. Progr. Rep. Inst. v. Perceptie Onderzoek, Eindhoven 1968.
- [8] Cardozo, B. L., The perception of jittered pulse trains. In: Frequency analysis and periodicity detection in hearing (Ed.: Plomp, R. and Smoorenburg, G. F.). A. W. Sijthoff, Leiden 1970.
- [9] Friedlander, F. G., On the oscillations of the bowed string. *Proc. Cambridge Phil. Soc.* **49** [1953], 516.
- [10] Lazarus, H., Die Behandlung der selbsterregten Kipp-schwingungen der gestrichenen Saite mit Hilfe der endlichen Laplacetransformation. Dissertation, Techn. Univ. Berlin 1972. Also: Cremer, L., Die Geige aus der Sicht des Physikers. *Nachr. Akad. Wiss. Göttingen: II Math. Physik. Kl.* **12**<sup>1</sup> [1971], 223.
- [11] Reinicke, W., Die Übertragungseigenschaften des Streichinstrumentensteges. Dissertation, Techn. Univ. Berlin 1973.
- [12] Fryxell, R. E., The structure of bow-hair. *Catgut Acoust. Soc. Newsl.* **20** [1973], 8. James, J., Jongebloed, W. L., and Molenaar, I., The role of hair structure in sound production of bowed instruments: a study with the light and scanning electron microscope. *Mikroskopie* **28** [1972], 298. Jolly, V. G., More about the structure of bow hair. *Catgut Acoust. Soc. Newsl.* **22** [1974], 20.
- [13] Cremer, L., Das Schicksal der "Sekundärwellen" bei der Selbsterregung von Streichinstrumenten. *Acustica*, **42** [1979], 133. See also: The absorption of "secondary correction waves" in the excitation of a string by bowing. *Catgut Acoust. Soc. Newsl.* **31** [1979], 12.
- [14] Keller, J. B., Bowing of violin strings. *Comm. Pure Appl. Math.* **6** [1953], 483.
- [15] Helmholtz, H., On the sensations of tone. Dover, New York 1954 (English translation of the German edition of 1877), pp. 80—88.
- [16] Saunders, F. A., Recent work on violins<sup>1</sup>. *J. Acoust. Soc. Amer.* **25** [1953], 491.
- [17] Rayleigh, J. W. S., The theory of sound. Dover, New York 1945, § 129.

<sup>1</sup> Republished in Benchmark Papers in Acoustics (series editor, R. Bruce Lindsay). Vols. **5**, **6**: Musical acoustics, violin family (edited by C. M. Hutchins). Wiley-Halsted, New York London 1975.

## **Aperiodicity in Bowed-String Motion: on the Differential-Slipping Mechanism**

In a recent article [1], we investigated ways in which the motion of a bowed string is observed to depart from exactly-periodic, Helmholtz-type motion. Three distinct kinds of departure were observed, and analyzed theoretically. We referred to these as flyback jitter, subharmonics, and spikes. The last-named phenomenon appears to be musically the most important. It accounts for the marked buildup of audible noise accompanying the musical note when a violinist plays more and more loudly with the bow near the bridge, and sets one of the practical limits on the "tolerance range" of usable bowing parameters.

The spikes in question appear in the waveform of transverse force exerted by the string on the bridge, whenever the noise builds up. A pair of typical waveforms is shown on the left of Fig. 1. The upper and lower traces correspond respectively to lighter and heavier bow force, and to softer and louder audible noise. For the lower trace the noise was well beyond normal limits of musical acceptability (although the limits of acceptability can of course vary with musical context). Changing the bow force changes the average tim-

ing and amplitude of the spikes. The timing of the main Helmholtz flybacks in both waveforms is by contrast closely periodic, and independent of bow force in the range considered. The spikes are the only strongly aperiodic feature, and are presumably the source of the noise.

A combination of simple theoretical arguments, computer simulations and laboratory experiments using hand-bowing led us to a clear identification of the physical mechanism producing the spikes, which turns out to depend on the finite width of the ribbon of bow-hair in contact with the string. The spikes are due to differential slipping, in which some but not all of the bow hairs release from time to time during the nominal "sticking" phase of the Helmholtz cycle. Unfortunately the comparisons amongst the experiments and computer simulations, as presented in [1], were irretrievably obscured by a printer's error in which two superficially similar experimental figures were interchanged, making nonsense of the degree of resemblance claimed in two key comparisons. The purpose of this note is to make the comparisons clear, by presenting the most pertinent figures correctly juxtaposed so that the extent of the resemblance can be appreciated.

The first of the two key comparisons was between experiments with an ordinary bow, and experiments with a

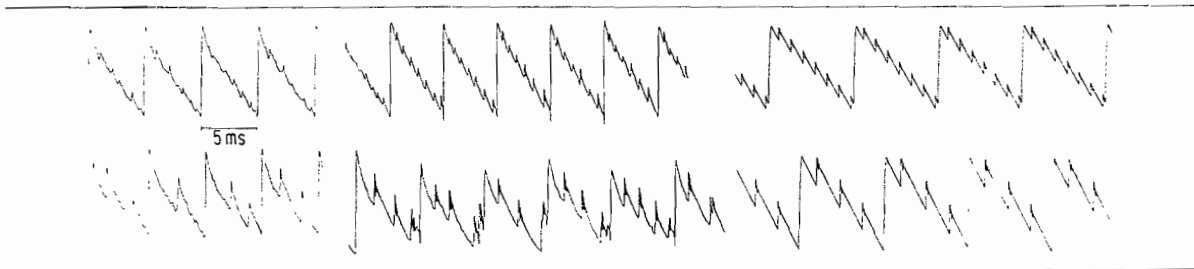


Fig. 1. Left: Bridge-force waveforms obtained by hand bowing with a normal bow on the open G string of a violin. The inner edge of the ribbon of bow-hair was at a distance from the bridge about two-thirds of the width of the ribbon. Upper trace is for lighter bow force, lower trace is for heavier. Centre: Bridge-force waveforms obtained with the double stick at a comparable position on the string, and with respectively similar values of bow force. Right: Simulated bridge-force waveforms under similar conditions. The two "bow-hairs" divide the string in the ratio 2:2:107. Bow force for the lower trace is 2.4 times that for the upper trace. For more detail see Figs. 18 d and 18 e of [1].

special "bow" having just two rigid "hairs" rather than the many, compliant hairs of a normal bow. The latter experiments were more amenable to theoretical analysis and computer simulation. We used a "double stick" made of polished wood having two thin, parallel ridges about 5.5 mm apart to which rosin was applied. Two examples of the resulting waveforms, obtained with both ridges of the double stick in contact with the string, under conditions qualitatively similar to those for the left-hand traces, are presented in the centre of Fig. 1. (These were misprinted as Fig. 20 in [1], which was interchanged with Fig. 16.) Spikes appear as before, albeit somewhat more regularly, but with just the same qualitative dependence of amplitude and timing upon bow force. A similar noise was audible against the musical note, varying similarly with bow force. The spikes and the noise both disappeared whenever either of the ridges lost contact with the string.

The second comparison was between these double-stick experiments and computer simulations, carried out using a two-bow-hair version of the efficient numerical model described in [2]. The simulated waveforms are exemplified by the right-hand pair of traces in Fig. 1, for which the values of bow force are qualitatively comparable to those in the experiments. Spikes again appear, recognizably similar albeit even more regularly spaced. The timing and amplitude of the simulated spikes again have the same qualitative behaviour, and the simulated string-velocity waveforms at the two "bow-hairs" (presented in [1]) provide a direct check that the spikes are indeed caused by slipping at just one bow hair (usually the one nearer the bridge), while the other hair sticks. A further check on the whole picture comes from simple order-of-magnitude estimates of the frictional forces at the two hairs ([1], sections 4.2. and 5.). The simulated spikes can be made less regular by introducing some random noise into the model friction characteristic, to mimic rosin irregularity.

Although the foregoing seems more than enough to identify differential slipping as the essential mechanism responsible for the spikes and their audible consequences

(see [1] for a more detailed discussion), it should be kept in mind that the comparison between the simulations and the double-stick experiments is not intended to be quantitative. This is because of the limitations of the experiments, in which bow force and bow position could not be controlled with sufficient precision, and in which the "corner-rounding functions" [2], characterizing the string and its terminations in the simulations, could not be measured accurately enough. It would require considerable experimental ingenuity to measure the corner-rounding functions accurately enough to permit a quantitative comparison between simulation and experiment, since both transverse and torsional string motion are involved and it is crucial to resolve transient behaviour on the very short time scales characteristic of the nonlinear bow-string interaction. In the present simulations torsional motion was suppressed altogether, even though it is computationally straightforward to include it.

(Received December 12th, 1981.)

M. E. McIntyre  
Dept. of Applied Mathematics  
and Theoretical Physics,  
University of Cambridge  
R. T. Schumacher  
Dept. of Physics, Carnegie-Mellon University,  
Pittsburgh, Pa. 15213  
J. Woodhouse  
Topexpress Ltd., 1 Portugal Place,  
Cambridge, England, CB5 8AF

#### References

- [1] McIntyre, M. E., Schumacher, R. T., and Woodhouse, J., Aperiodicity in bowed-string motion. *Acustica* **49** [1981], 13.
- [2] McIntyre, M. E. and Woodhouse, J., On the fundamentals of bowed-string dynamics. *Acustica* **43** [1979], 93.